A Recyclable Mineral Catalyst for Visible-Light-Driven Photocatalytic Inactivation of Bacteria: Natural Magnetic Sphalerite

ARTICLE *in* ENVIRONMENTAL SCIENCE & TECHNOLOGY · SEPTEMBER 2013

Impact Factor: 5.33 · DOI: 10.1021/es402170b · Source: PubMed

Environmental Science & Technology

Article

pubs.acs.org/est

A Recyclable Mineral Catalyst for Visible-Light-Driven Photocatalytic Inactivation of Bacteria: Natural Magnetic Sphalerite

Dehua Xia,[†] Tsz Wai Ng,[†] Taicheng An,*[,‡] Guiying Li,[‡] Yan Li,[§] Ho Yin Yip,[†] Hunjun Zhao,[∥] Anhuai Lu,[§,⊥] and Po-Keung Wong*[,†]

[†]School of Life Sciences, The Chinese University of Hong Kong, Shatin, NT, Hong Kong SAR, China

[‡]State Key Laboratory of Organic Geochemistry, Guangzhou Institute of Geochemistry, Chinese Academy of Sciences, Guangzhou 510640, China

[§]The Key Laboratory of Orogenic Belts and Crustal Evolution, School of Earth and Space Sciences, Peking University, Beijing 100871, China

[∥]Centre for Clean Environment and Energy, Gold Coast Campus, Griffith University, Queensland 4222, Australia

[⊥]School of Geoscience and Info-Physics, Central South University, Changsha 410083 China

Supporting Information

ABSTRACT: Motivated by recent studies that well-documented mineral photocatalyst for bacterial inactivation, a novel natural magnetic sphalerite (NMS) in lead−zinc deposit was first discovered and evaluated for its visible-light-driven (VLD) photocatalytic bactericidal properties. Superior to the reference natural sphalerite (NS), vibrating sampling magnetometeric (VSM) analysis revealed the ferromagnetic property of NMS, indicating its potential for easy separation after use. Under the irradiation of fluorescence tubes, NMS could inactivate 7 $\log_{10}$ Gram-negative *Escherichia coli* K-12 without any regrowth and metal ions leached out from NMS show no toxicity to cells. The cell destruction process starting from cell wall to intracellular components was verified by TEM. Some products from damaged cells such as aldehydes, ketones and carboxylic acids were identified by FTIR with a decrease of cell wall functional groups. The relative amounts of potassium ion leakage from damaged cells gradually increased from initial 0 to approximately constant concentration of 1000 ppb with increasing reaction time. Superoxide radical ($\bullet O_2^-$) rather than hydroxyl radical ($\bullet$OH) was proposed to be the primary reactive oxidative species (ROSs) responsible for *E. coli* inactivation by use of probes and electron spin resonance (ESR). H_2O_2 determined by fluorescence method is greatly involved in bacterial inactivation in both nonpartition and partition system. Multiple cycle runs revealed excellent stability of recycled NMS without any significant loss of activity. This study provides a promising natural magnetic photocatalyst for large-scale bacterial inactivation, as NMS is abundant, easily recycled and possessed an excellent VLD bacterial inactivation ability.

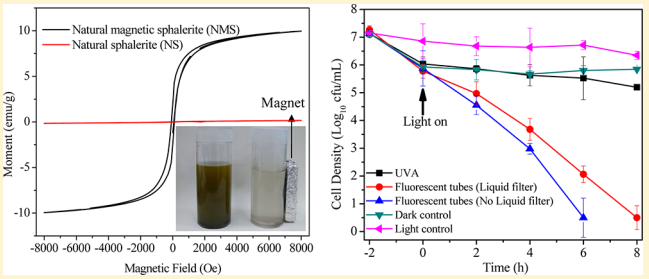

INTRODUCTION

Naturally occurring semiconductor minerals are earth-abundant and able to perform as visible-light-driven (VLD) photocatalyst for environmental remediation based on recent studies.[1−7] The VLD photoactivity of these materials is due to the various impurity elements and complicated crystal lattice defects.[3] Until now, several kinds of natural semiconductors like rutile and sphalerite have been successfully applied to reduce heavy metal, to degrade azo dyes, and to decompose halohydrocarbons under VL irradiation.[1−6] Specially, natural sphalerite (NS) collected from Huangshaping deposit could totally inactivate 7 $\log_{10}$ *Escherichia coli* K-12 within 6 h under irradiation of fluorescence tubes (FTs), owing to the major effect of conduction band e^-, directly inject into bacteria and lead to the irreversible damage of cell.[6,7] Compared with frequently reported VLD photocatalysts that are tedious in fabrication procedure, and expensive for massive production, natural VLD minerals readily obtained with lower cost and have a great potential in cost-effective environmental applications. Nevertheless, difficulty in separation and recycling of these materials may still hinder their large-scale application in some content.

Magnetically separable photocatalysts have attracted increasing attention due to their efficient recycle effect in water treatment and purification system, because filtration and centrifuge are costly and tedious.[8−12] Strategies to synthesize magnetically VLD photocatalysts tend to be limited for application, as most of which are suffered dramatically decrease of photocatalytic activities and poor stability, such as $Fe_2O_3/SiO_2/TiO_2$, $TiO_2/ZnFe_2O_4$, etc.[9−12] In the present study, a

Received: May 15, 2013
Revised: July 23, 2013
Accepted: September 6, 2013
Published: September 6, 2013

novel natural magnetic sphalerite (NMS) from lead−zinc mine in China was found and utilized directly as an effective recyclable VLD photocatalyst for bacterial inactivation. It is worthwhile to note the differences of NMS from the previously reported NS: first, VSM analysis showed that the specific ferromagnetic property only existed in NMS rather than NS, making NMS possess great potential for materials recycle; second, unlike NS,[3] chemical composition of NMS can be expressed as $(Zn_{0.856}Fe_{0.169}Cu_{0.0004})_{1.0254}S$ based on electron microprobe analysis (EMPA) results, revealing good coherence with doped ZnS and complicated crystal lattice defect of NMS, while NS is $(Zn_{0.732}Fe_{0.284}Cu_{0.043}Ni_{0.003}Ag_{0.003}Cd_{0.002}Mn_{0.002}Co_{0.001})_{1.070}S$; third, UV−vis DRS test display narrower band structure (2.03 eV) for NMS than NS (2.24 eV), indicating better VL adsorption ability. It is reasonable to infer that specific property of NMS may impose new variables to its VLD photocatalytic processes from NS. A study of photocatalysis by NMS is therefore necessary for evaluating its practical applications such as development of a natural magnetic photocatalyst-based disinfection technique.

In the present study, fluorescence tubes (FTs) have been employed by virtue of its low cost, long life-span and safety.[6,7,13] The photocatalytic inactivation of *E. coli* in an aqueous NMS suspension under FTs was systematically studied from the mechanistic and kinetic viewpoints. Besides, many reports proposed the photocatalytic degradation of the cell structure leads to cell death under visible light. Saito et al.[14] used potassium ion leakage as a criterion for measuring cell membrane damage; Nadtochenko et al.[15−17] found the photocatalytic degradation of lipo-polysaccharide, phosphatidylethanolcholine, and peptidoglycan, which are the main wall structure elements by ATR-FTIR identification; Maness et al.[18] proposed that the loss of the membrane structure was the root cause of cell death. Thus photocatalytic degradation of the cell envelope was characterized by TEM and FT-IR measurements in our study. The merits of NMS coupled with continuous operating FTs are promising for the photocatalytic bacterial inactivation, and will probably be an economically viable solution to wastewater treatment and water disinfection.

EXPERIMENTAL SECTION

Materials. The natural magnetic sphalerite (NMS) used in this study, collected from a lead−zinc mine in China, was obtained after screening a large number of NS samples from mining sites. After mechanically crushed and milled at the mine, the resultant particles were then passed through sieve pores to obtain sphalerite powder with particle sizes <38 μm. X-ray diffraction (XRD) pattern of NMS was recorded using a DMAX-2400 (Rigaku, Japan, Cu Kα, λ = 0.15406 nm) with a secondary graphite crystal monochromator. Chemical composition of the NMS was obtained using a JXA 8100 electron microprobe analysis (EMPA, JEOL, Japan) with a 15 KV acceleration voltage and 10 nA beam current. UV−vis spectrophotometer (Lambda 950) with an integrating sphere from 300 to 800 nm was used to record UV−vis diffuse refelection spectrum (DRS) of NMS. The surface morphology of NMS was observed on transmission electron microscopy (TEM, FEI Tecnai G2 Spirit). The magnetic properties of the NMS powder was determined by vibrating sample magnetometer (VSM-7300, Quantum design, Lakeshore, USA) at 25 °C. In contrast, tests for physio-chemical features of natural sphalerite (NS) samples were also conducted.

Photocatalytic Inactivation. A representative bacterial type of Gram-negative *Escherichia coli* K-12, commonly used as faecal contamination indicator microorganism, was chosen as model bacteria for the treatment. A suspension (50 mL) containing NMS and *E. coli* K-12 in a flask was placed in a black box (20 cm width, 80 cm length, and 50 cm height) and vigorously stirred by a plastic stirrer at suitable velocity. The commonly household lightening source, fluorescent tubes (15 W, VELOX, Thailand), were applied as light source and placed in the back side of reactor (Supporting Information (SI) Figure S1). The VL and UV intensities inside the flask were measured by a light meter (LI-COR, Lincoln, Nebraska, USA) and an UVX digital radiometer (UVP, Upland, California, USA), respectively. A liquid filter (5 mol/L sodium nitrite) was placed between the FTs and the flask to block all UV emission. All glassware used in the experiments was washed with deionized (DI) water, and then autoclaved at 121 °C for 20 min. *E. coli* K-12 was inoculated in 50 mL nutrient broth (Lab M, Lancashire, UK) at 37 °C for 16 h in a shaking incubator. The bacteria were harvested by centrifugation in an eppendorf tube at 10 000 rpm for 4 min and washed twice with sterilized saline (0.9% NaCl) solution, and then resuspended in sterilized saline solution. The final cell density was adjusted to about 2×10^7 cfu (colony forming unit)/mL in the reaction mixture. At different time intervals, stirring was stopped first, then aliquots of the sample was collected and serially diluted with sterilized saline solution. 0.1 mL of the diluted sample was immediately spread on nutrient agar (Lab M, Lancashire, UK) plates and incubated at 37 °C for 24 h to determine the survival number of cells (in cfu) by plating them on agar plate. The setup of the partition system for this experiment is shown in SI Figure S2. In this system, semipermeable membrane compartment with 20 mL *E. coli* K-12 suspension (2×10^7 cfu/mL) was bind to the plastic stirrer, then immerse in the 50 mL even-distributed NMS suspension and rotate with the stirrer. At different intervals, aliquots of cells inside the membrane were sampled and immediately diluted, following the same procedure as described in the nonpartition system. For comparison, dark (NMS and bacterial cells without light), light (bacterial cells and light without NMS) and negative controls (bacterial cells alone) were also conducted. All treatments and control experiments were performed in triplicate.

Fluorescence Spectroscopy. The NMS and *E. coli* K-12 mixture before and after photocatalytic treatment was collected and stained with the dyes of LIVE/DEAD BacLight bacterial viability kit (L7012, Molecular Probes, Inc., Eugene, OR) following the procedure recommended by the manufacturer. After being incubated at 25 °C in the dark for 15 min, the samples were transferred to the coverslip and examined using a fluorescence microscopy (Nikon ECLIPSE 80i, Japan) equipped with a filter block NUV-2A consisting of excitation filter Ex 400−680 (Nikon, Japan) and Spot-K slider CCD camera (Diagnostic instruments. Inc., Sterling Heights, MI).

Transmission Electron Microscopy (TEM). The mixture comprising the NMS and *E. coli* K-12 before and after the photocatalytic reaction was collected and centrifuged. The bacterial cells were prefixed by 2.5% glutaraldehyde and trapped in 3% low melting point agarose. After being postfixed by 1% osmium tetraoxide (E.M. grade, Electron Microscopy Sciences, Fort Washington, PA) in phosphate buffer (0.1 M, pH 7.2), the cell pellet was dehydrated by adding a series of ethanol with graded concentration and finally embedded in spurr solution (Electron Microscopy Sciences, Fort Washington, PA) for

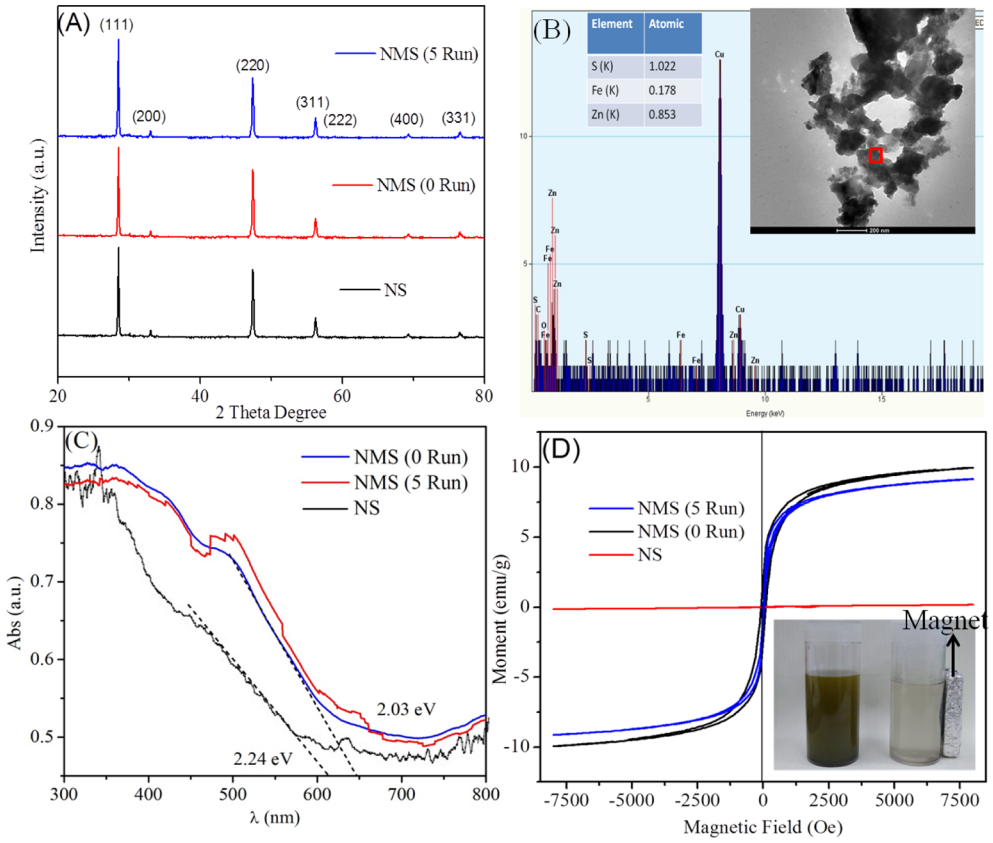

Figure 1. Characteristics comparison of NMS and NS samples. (A) XRD, (B) TEM-EDX (Inset: TEM morphology of NS), (C) UV−vis DRS, (D) magnetic hysteresis loops.

polymerization at 68 °C. Then samples were cut into 70 nm ultrathin sections by using an ultramicrotome (Leica, Reichert Ultracuts, Wien, Austria), and further stained with uranyl acetate and lead citrate on copper grids. Finally, the stained ultrathin sections were observed by a JEM-1200 EXII transmission electron microscope (JEOL Ltd., Tokyo, Japan), following the reported references.[6,7,13]

Analysis of Leakage of Ions and Bacterial Catalase Activity. To investigate the metal ion bleached from NMS and potassium ion (K^+) leakage from bacterial cells during the photocatalytic inactivation process, the mixture before and after treatment was collected and filtered through a Millipore filter (pore size of 0.45 μm, Spectrum Laboratories, Rancho Dominguez, Canada).[6,13] After filtration, the concentration of metal ions was measured by a polarized Zeemanatomic atomic absorption spectrophotometer (AAS) (Hitachi Z-2300, Japan). Catalase (CAT) activity assay was conducted using the Catalase Assay Kit (Cayman Chemical Company, Ann Arbor, MI), following the protocol recommended by the manufacturer. One unit of CAT activity (nmol/min/mL) was defined as the amount of enzyme that would cause the formation of 1 nmol formaldehyde/min at 25 °C.[6,13]

Fourier Transform Infrared (FT-IR) Spectroscopy. A FTS-4000 Varian Excalibur Series FTIR spectrometer with attenutated toral refelection (ATR) (Varian, Palo Alto, CA) was used to collect the infrared spectra. Spectra from 4000 to 800 cm^{-1} were collected with a resolution of 4 cm^{-1}, and the ordinate was expressed as absorbance. Each spectrum was an average of 256 scans with automatic baseline correction. Samples were prepared by the following procedure: the suspensions at different reaction times were evaporated by a freeze-drying method, then the dry residue was supported on KBr pellets for FTIR measurement.[15−17]

RESULTS AND DISCUSSION

Photocatalytic Inactivation Performance. NMS particle is in a pure phase of cubic sphalerite with a 2.01 eV calculated band gap (Figure 1), the typical chemical formula of NMS can be expressed as $(Zn_{0.856}Fe_{0.169}Cu_{0.0004})_{0.972}S$ (Table 1), indicating its good coherence with doped ZnS and excellent potential VLD photoactivity. The detailed differences and comparison of physio-chemical features between NMS and NS are discussed in the SI. Figure 2A displays the VLD photocatalytic inactivation efficiencies of Gram-negative *E. coli* K-12 by NMS. The optimal concentration of the photocatalyst was optimized as 1 g/L (SI Figure S4). Light control was carried out in the absence of any NMS under FTs irradiation, and the bacterial population remained essentially unchanged after 6 h suggesting no photolysis happen to *E. coli* K-12. In the dark controls, the bacterial population first reduces almost 1.5 log after 2 h stirring, and then no further reduction of bacterial population was observed. This phenomenon may attribute to the establishment of adsorption−desorption equilibrium between NMS particles and bacterial cells. Actually, mechanically ground and naturally bearing impurities caused many heterogeneous surface defects which may benefit the adsorption of *E. coli* K-12 cells to the NMS surface.[3−5] After attained saturation adsorption between NMS and bacterial cells, the mixture solution were then irradiated by VL, and the bacterial population decreased with time until total inactivation of *E. coli* K-12 was observed after 6 h treatment.

dx.doi.org/10.1021/es402170b | *Environ. Sci. Technol.* 2013, 47, 11166−11173

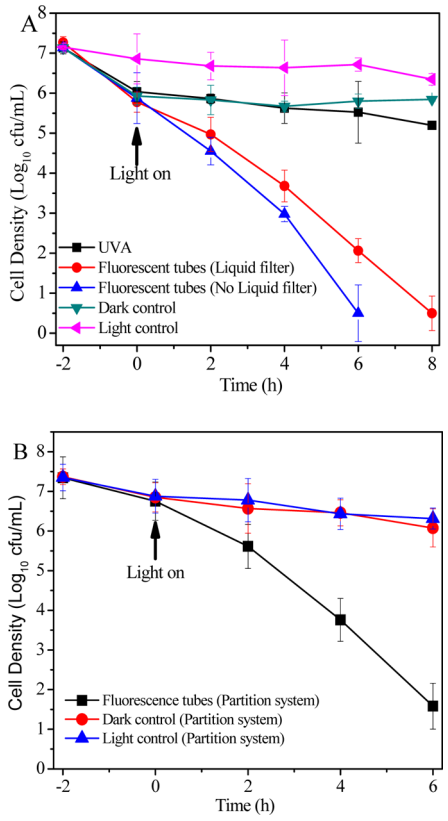

Figure 2. Photocatalytic inactivation efficiency against *E. coli* K-12 (2×10^7 cfu/mL, 50 mL) in the presence of NMS under VL irradiation (without and with liquid filter). (A) Nonpartition system, (B) Partition system. Experimental conditions: fluorescent tubes without filter (visible light intensity = 3.58 mW/cm^2, UVA intensity = 0.03 mW/cm^2, UVB intensity = 0.005 mW/cm^2 and UVC intensity = 0.002 mW/cm^2); fluorescent tubes with liquid filter (visible light intensity =2.7 mW/cm^2, no UVA, UVB, and UVC); UVA lamp (UVA intensity = 0.03 mW/cm^2, UVB intensity = 0.05 mW/cm^2, and UVC intensity = 0.01 mW/cm^2).

Fluorescent tube (FT) can emit not only VL ($\lambda \geq 400$ nm) but also small amounts of UV ($\lambda \leq 380$ nm). To further confirm that NMS is a true VLD photocatalyst and the bactericidal effect of *E. coli* K-12 is due to the VL photocatalysis, a sodium nitrite (5 mol/L) liquid filter is installed between fluorescence tubes and reactor flask to cut off UV. Under this condition, the intensity of VL decreased to 2.9 mW/cm^2 and no UV was detected. A complete inactivation of *E. coli* K-12 was achieved with prolonged 8 h irradiation (Figure 2A). Based on the inactivation levels of FTs exposure with and without UV cutoff, it is noteworthy that NMS is indeed a VLD photocatalyst and the observed inactivation primarily resulted from the VL irradiation. In contrast, UVA lamp with same UV intensity of FTs (intensity adjusted by changing the distance between lamp and flask), also be used as the only light source to study the effect of UV to the photocatalysis of NMS, which showed an approximately 0.5 $\log_{10}$ reduction of inactivation level, indicating UV photocatalysis is not important contribution to the inactivation of this bacteria in this system.

To determine whether the reaction occurs on the surface of NMS or in the bulk solution, the partition system was employed. In this case, the molecular weight cutoff (MWCO) of semipermeable membrane is $12-14 \times 10^3$ dalton (pore size = 5 nm), whereas the rod-shaped *E. coli* K-12 cell is about 2.6×10^6 dalton (diameter = 500 nm) and the diameter of NMS is less than 38 μm, so that the direct contact was prohibited as both species cannot pass through the membrane.[19] Figure 2B shows the inactivation efficiency of *E. coli* K-12 inside the membrane container. For the controls, due to the membrane cutoff effect, only 0.6-log reduction of cell population was observed after 8 h stirring, which caused by the adsorption of membrane,[6,19] indicating no toxic effect of light or membrane to the cells. These controls reveal the cell density decrease is not as significant as in the nonpartition system (1.5 $\log_{10}$), give another solid evidence to prove that the decrease of cell in nonpartition system is due to adsorption. Interestingly, only 5.2 $\log_{10}$-reduction of *E. coli* K-12 was observed when the outer system was irradiated by VL, the inactivation level was a little lower than that without membrane, indicating the inactivation process was partially inhibited and direct contact was important in the NMS-VL system.

To further confirm the bactericidal effect of NMS-FTs system, the BacLight kit fluorescent microscopic method was conducted in accordance with reported references.[19,20] Notably, NMS could not been stained by both dyes, which emit no fluorescence but in a primitive brown bulk (Figure 3A). Figure 3A further proves the adsorption between cells and NMS, it presents that the stained viable cells in green color bind firmly to the brown NMS particle. Figure 3B shows the viable cells with intense green fluorescence. After being photocatalytically treated for 1 h, some cells turned to red fluorescence, indicating some bacteria was cracked and intracellular component was released (Figure 3C). With prolonged irradiation time, fewer and no living bacterial cells were observed respectively after 4

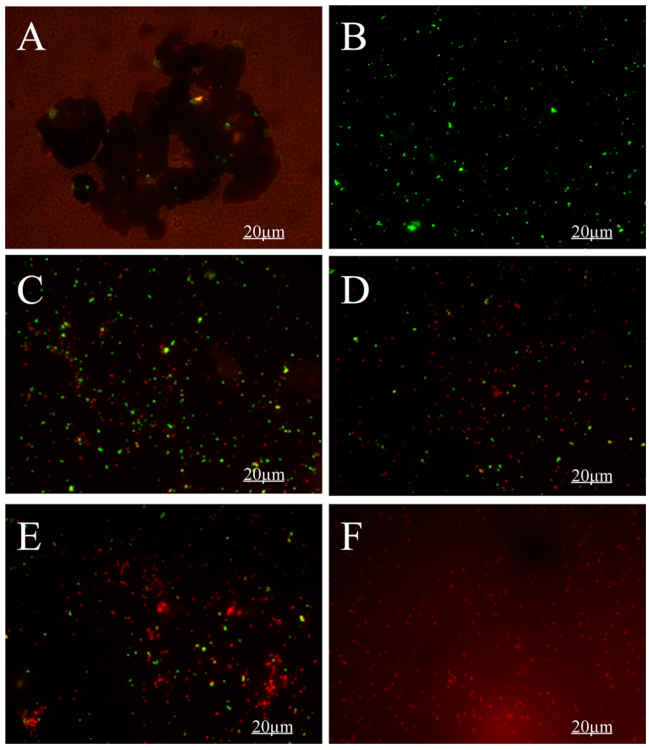

Figure 3. Fluorescence microscopic images of *E. coli* K-12 (2×10^7 cfu/mL, 50 mL) photocatalytically untreated or treated in the presence of NMS (50 mg) under VL irradiation. (A) NMS, (B) The mixture of NMS and *E. coli* K-12 before irradiation, and after irradiation by VL for (C) 1, (D) 2, (E) 4, and (F) 6 h.

and 6 h (Figure 3E and F), more red stained intracellular DNA and protein came out and even aggregated together. In fact, only about maximum 10 colonies of bacterial cell were still survivals, according to the inactivation data of Figure 2A. On the basis of above results, it can conclude that NMS performed excellent VLD photocatalytic inactivation effect.

In conclusion, similar with the reference NS, present results showed that photogenerated ROSs from NMS-FTs system could effectively inactivate representative bacteria. The original excellent VLD activity should be attributed to the good coherence of doped ZnS and complicated crystal lattice defect in NMS, based on the physiochemical analysis (SI Table S1, Figure 1). It is well-known that pure ZnS and sphalerite are wide band gap semiconductors (~3.5−3.7 eV and ~3.6 eV, respectively), but FeS possesses a very narrow band gap (~0.1 eV) and CuS has no band gap at all.[21] These substituting metal ions in NMS could introduce more electron donor states, also reduce the bandgap and help broaden the absorbing edge toward the visible light. More importantly, Figure 1D illustrates the representative magnetic hysteresis loops of NMS, with about 9.8 emu/g saturation magnetization, suggesting a typical ferromagnetic behavior and soft magnetic feature with less coercivity and remanence, while the saturation magnetism of NS could be negligible.[8−11,22,23] Superior to NS, these typically soft magnetic NMS can be easily magnetically separated from water, which is desirable for their applications considering its dispersion and recycle (Inset of Figure 1D).[11,22,23]

Destruction of Bacterial Cells. To better understand the destruction of bacterial cells in the present system, the microstructure and morphology of *E. coli* K-12 at different stages of photocatalytic inactivation was identified by TEM (Figure 4). Figure 4A shows a representative TEM image of

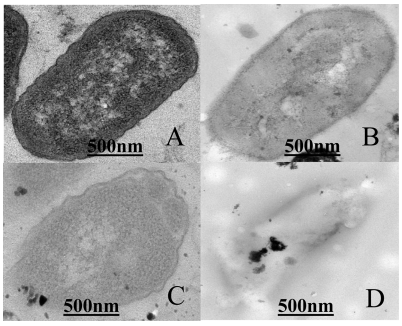

Figure 4. TEM images of *E. coli* K-12 photocatalytically untreated or treated with NMS under VL irradiation. (A) 0 h, (B) 6 h, (C) 12 h, and (D) 30 h.

untreated *E. coli* K-12, which exhibited evenly rendered interior of the cell with a well-preserved cell wall. After 6 h, the central portion of the cell was still intact but part of the cell wall appeared obscure, indicating initial damage to the outer membrane and leading to a leakage of the interior component. Obviously, great damage in the structure of *E. coli* K-12 was observed after 12 h, the cell wall became greatly ruptured and the interior component was severely lost. Finally, the whole cell became translucent, and finally was totally decomposed after 30 h, leaving only fragmented cell debris. This observation suggests that the destruction process of the bacterial cell is to begin from cell envelope to the inner cellular components. Due to the critical role of direct contact between bacterial cell and NMS, the first attack site is expected to be the cell envelope. Till the outer envelope is ruptured, accompanied with the degradation of cytoplasmic components.

Potassium ion (K^+), an important component in bacteria and involving in the regulation of polysome content and protein synthesis. Its leakage was as a criterion to measure cell membrane damage,[14] and immediately leaked out from injured cells was observed because of the permeability change in the envelope. The relative amount ($C-C_0$) of K^+ leakage gradually increased from initial 0 ppb, then reaching an approximately stable value of 1000 ppb at the end of reaction, which was in parallel with the inactivation process with increasing irradiation time (SI Figure S5). In comparison, no significant leakage of K^+ occurred in the control experiments. This result suggested that the cell membrane permeability had been discrupted with the inactivation of *E. coli*.

FT-IR Spectra Change of *E. coli* Treated with NMS. FTIR provides a means to identify key functional groups and structures of the cells, and evaluate changes of cells caused through exposure to photocatalysts.[15−17] Figure 5 shows FT-IR

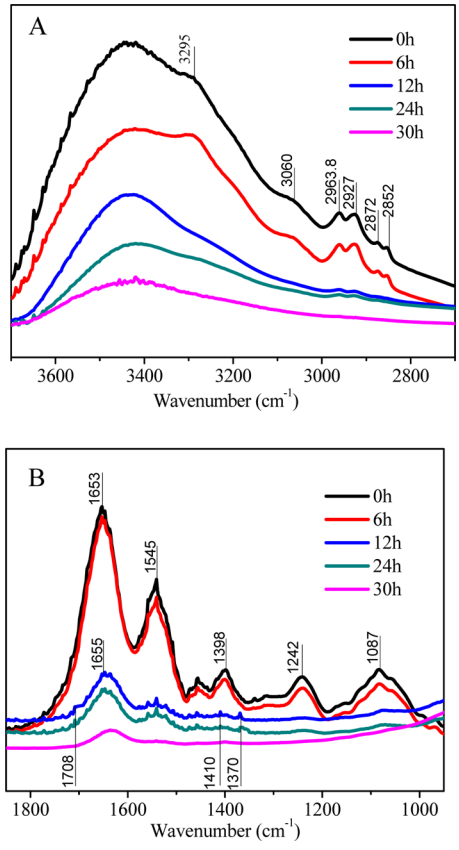

Figure 5. Changes of FT-IR spectra of *E. coli* K-12 during the photocatalytic inactivation with NMS. (A) Bands in the spectral region of 3700−2500 cm^{-1} and (B) bands in the spectral region of 1850−950 cm^{-1}.

spectras of *E. coli* K-12 as a function of time during VLD photocatalysis by NMS, the specific functional groups were identified by referencing the reported values for biomolecules and bacteria cells.[15−17] In Figure 5A, the characteristic peaks at 3295 and 3060 cm^{-1} were attributed to amide A and amide B, respectively, while the peaks at 2963, 2927, 2872, and 2852 cm^{-1} were assigned to ν_a (CH_3), ν_a (CH_2), ν_s (CH_3), and ν_s (CH_2), respectively. A wide skewed band in the region 3400−3600 cm^{-1} due to the OH^- vibrations of the absorbed water

dx.doi.org/10.1021/es402170b | Environ. Sci. Technol. 2013, 47, 11166−11173

and OH^- on the NMS surface. With increasing reaction time, the intensity and integral absorbance of these initial *E. coli* K-12 spectral profile quickly disappeared or decayed. After 30 h, the disappearance of amide A (3295 cm^{-1}) and amide B (3060 cm^{-1}) were observed, and also the peak intensity of the C−H bands (2963, 2927, 2872, and 2852 cm^{-1}) were almost undetectable. Concomitantly, the wide band containing OH^- vibrations is transformed to a skewed form with a maximum at around 3460 cm^{-1}. Figure 5B shows significant changes of the initial oligosaccharide bands around 1087 cm^{-1}, and profile changes of the PO_2^- band near 1242 cm^{-1}, as well as the decay of the amide I band near 1653 cm^{-1} and the amide II band near 1545 cm^{-1}. In parallel, an increase in absorbance in the region related to the C═O bonds of aldehydes and ketones between 1690 and 1734 cm^{-1} was seen. After 12 h, the prominent peaks at 1410 and 1370 cm^{-1} were also observed due to the increase in the concentration of carboxylic groups, indicating the formation of carboxylic acid with the photocatalytic degradation of the cell membrane. SI Figure S6 shows the results of control experiments without NMS. No formation of carboxylic acid occurred as no carboxylic groups' peak appeared at 1370 cm^{-1} in the FTIR spectra of *E. coli* K-12 and only small decrease in amide I and amide II bands were detected, indicating almost no changes of *E. coli* K-12 after 30 h irradiation. The results revealed that the cell wall and membrane of bacteria were decomposed by the oxidation of the reactive species rather than photolysis of bacteria, resulting in the cell death.

Stability and Recycle of NMS. The stability of NMS was investigated by repeating photocatalytic inactivation of *E. coli* K-12 experiments with recycled NMS. After magnetic recycled by an magnet, the used NMS was then washed twice with distilled water and ethanol after first run photocatalytic treatment before another run. A slightly decrease of inactivation efficiency in the fifth run was observed, indicating the excellent stability of NMS without any significant loss of activity (Figure 6A). Fortunately, no significant differences were observed in the XRD and UV−vis DRS patterns of fresh and recycled NMS samples (Figure 1A, 1C), indicating the physicochemical features of NMS were still maintained even after 5 runs test. Moreover, only a little decrease of saturation magnetism was observed in the recycled NMS, which may be caused by the residual cell debris on the surface of NMS (Figure 1D). However, superior to NS and other artificial magnetic photocatalysts,[8−11,23] it still can be easily magnetic recycled.

However, the photocorrosion of Zn^{2+} may happen from metal sulfide such as ZnS and CdS after photocatalytic reaction.[24,25] In our case, when NMS was used as VLD photocatalyst, only a little amount elution of Zn^{2+} (0.17 mg/L) and Fe^{2+} (0.032 mg/L) can be detected by AAS when NMS was immerged in bacterial cells suspension within the 8 h experimental time scale, other metal impurity were undetectable (Figure 6B). Li et al.[21] also found that after 9 h irradiation by a 500 W tungsten halogen lamp, the Zn atom percentage on NS surface decreased from 27.5 to 24.4%, corresponded to a loss of 3.1% of the ZnS particles. As photocorrosion occurred to such a minor extent, the stability of NMS is considerable. Moreover, it is noteworthy to mention that no obvious bactericidal effect occurred after 8 h stirring (the first 2 h in dark, then 6 h under VL) in the presence of equal dosage of eluted Zn^{2+} or/and Fe^{2+}. The results further suggest that the decrease of 1.5 log cells of dark control should be resulted from the adsorption and NMS has no toxic effect on bacterial cells.

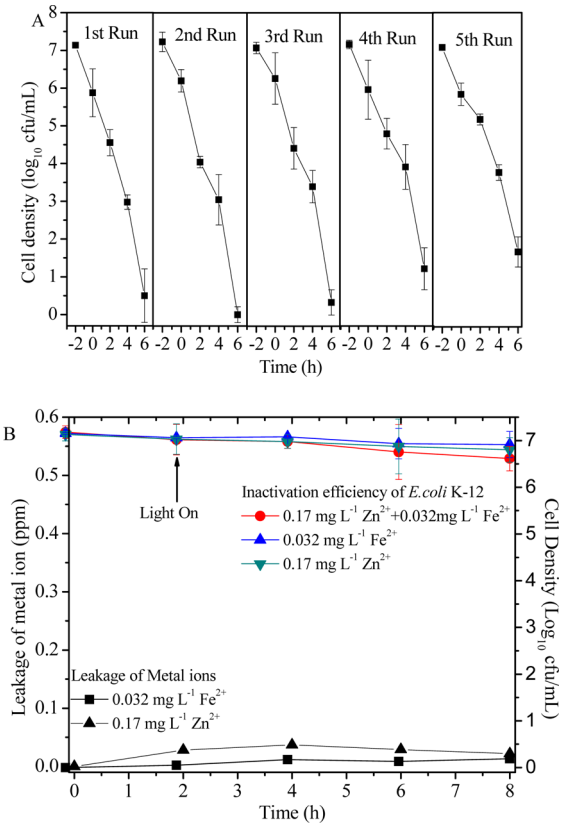

Figure 6. (A) Repeated experiments of photocatalytic inactivation of *E. coli* K-12 (2×10^7 cfu/mL, 50 mL) by NMS under VL irradiation, (B) Metal ion leakage from NMS, and *E. coli* K-12 inactivation in aqueous solution with addition of the equal amount of Zn^{2+} and/or Fe^{2+} leaked from NMS.

Analysis of ROSs Generation. To achieve the solid evidence of generated ROSs in the NMS-VL system, the ESR spin-trap with DMPO technique was also employed to obtain signals of other short-life span active radicals. No characteristic peaks corresponding to DMPO-•OH adducts were observed in both irradiated and unirradiated conditions (Figure 7A). Similarly, no obvious peaks were observed by fluorescence method using terephthalic acid as the •OH-trap agent (SI Figure S7), further confirming •OH is really not significant involved in the reaction. The results is consistent with the condition in theory that the VB-holes of NMS, elevated by the substitution of Zn with transition metal of Fe and Cu (VB for pure sphalerite is 2.2 V vs NHE, thus VB for NMS is less than 2.2 V), may could not oxidize the OH^-/H_2O to produce •OH (E^0 (OH^-/•OH)) = 2.38 V vs NHE).[19,26] However, the six characteristic peaks of the DMPO-•O_2^-adducts were observed under VL (Figure 7B), and no signals in dark, further confirming the formation and significant role of •O_2^- in this system. This is probably due to the CB-electrons of NMS have more negative potential (−1.4 V vs NHE) to reduce the surface chemisorbed O_2 to produce •O_2^- ($E^0(O_2/\bullet O_2^-)$) = −0.33 V vs NHE).[19,27] XTT sodium salt (0.15 mM), a probe for •O_2^-, as indicated by increase of absorption at 480 nm due to the formation of purple-colored product after photocatalytic degradation, was also observed.[28]

H_2O_2 production was determined by the microplate fluorometric method[29] (Figure 7C) both in partition and nonpartition system. The similar pattern was both obtained

dx.doi.org/10.1021/es402170b | Environ. Sci. Technol. 2013, 47, 11166−11173

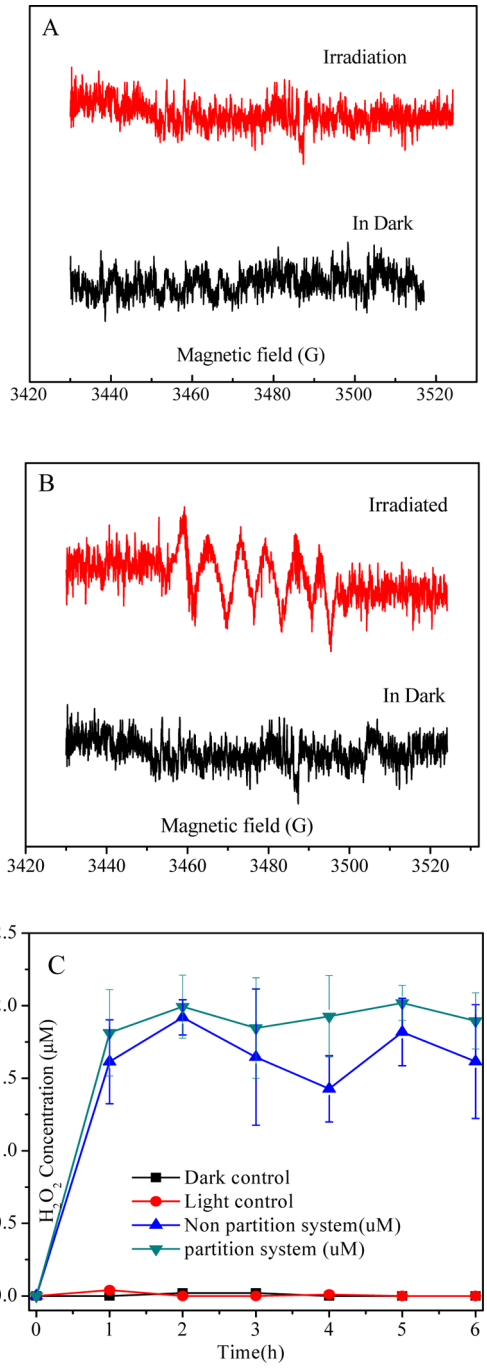

Figure 7. DMPO spin-trapping ESR spectra recorded at ambient temperature in NMS suspension under VL irradiation: (A) For DMPO-•OH in aqueous dispersion, and (B) For DMPO-$•O_2^-$ in methanol dispersion; (C) Accumulation of H_2O_2 produced in the presence of NMS (1 g/L) under VL irradiation.

that the concentration of H_2O_2 quickly increase and become stable with prolonged irradiation time. Interestingly, a little higher concentration of H_2O_2 was observed in the partition system, partly attributed to the fact that membrane-trapped residual RSs like •OH and $•O_2^-$ would enhance the transformation of H_2O_2, or it need longer diffusion time for H_2O_2 to transverse the membrane into the inner compartment. In such a case, noting that the total amount of H_2O_2 is much more than the actually measured equilibrium value of 1−2 μM, because H_2O_2 was generated continuously and dynamically consumed in situ in the system.[7] In CB, H_2O_2 is believed to be produced by the reduction or disproportionation of $•O_2^-$, whereas in VB H_2O_2 is formed by the coupling of two •OH too.[30−32] As mentioned, $•O_2^-$ rather than •OH plays more important role in the reaction, thus the primary origin of H_2O_2 should be from $•O_2^-$ generated from CB. To further confirm attacking effect of H_2O_2, the activity change of catalase (CAT), a well-known antioxidant enzyme that defends against oxidative stress from H_2O_2, was determined during inactivation of bacteria. In the beginning, CAT activity is found to be increased with irradiation time (SI Figure S8), suggesting a considerable amount of H_2O_2 was accumulated and the bacterial defense system quickly induces a higher level of CAT. After that, *E. coli* inactivation was accompanied by decreased CAT activity, while the inactivation rate is rapidly increasing, indicating the oxidative stress far beyond the protection ability of the bacterial enzyme system.[7] Moreover, the critical role of $•O_2^-$ and H_2O_2 in the photocatalytic inactivation process were further proved by the scavenger study (SI Figures S9−S12) and discussed in the SI.

■ ASSOCIATED CONTENT

Ⓢ Supporting Information

Additional detail information including setup of nonpartition and partition system, EMPA results of NMS, the optimization of NMS, CAT activity, FTIR of light control, fluorescence emission spectrum, and scavenger experiments. This material is available free of charge via the Internet at http://pubs.acs.org/.

■ AUTHOR INFORMATION

Corresponding Authors

*(T.A.) Phone: +86 20 85291501; fax: +86 20 8529 0706; e-mail: antc99@gig.ac.cn.

*(P.K.W.) Phone: +852 3943 6383; fax: +852 2603 5767; e-mail: pkwong@cuhk.edu.hk.

Notes

The authors declare no competing financial interest.

■ ACKNOWLEDGMENTS

The project was supported by a research grant (GRF476811) of the Research Grant Council, Hong Kong SAR Government to P.K.W., a research grant (NSFC21077104) of National Science Foundation of China to G.Y.L. and T.C.A, and a research grant of National Natural Science Foundation of China to A.H.L. (41230103) and Y.L. (41272003).

■ REFERENCES

(1) Lu, A. H.; Li, Y.; Lv, M.; Wang, C. Q.; Yang, L.; Liu, J.; Wang, Y. H.; Wong, K. H.; Wong, P. K. Photocatalytic oxidation of methyl orange by natural V-bearing rutile under visible light. *Solar Energy Mater. Solar Cells* **2007**, *91* (19), 1849−1855.

(2) Lu, A. H.; Liu, J.; Zhao, D. G.; Guo, Y. J.; Li, Q. R.; Li, N. Photocatalysis of V-bearing rutile on degradation of halohydrocarbons. *Catal. Today* **2004**, *90* (3−4), 337−342.

(3) Li, Y.; Lu, A. H.; Wang, C. Q.; Wu, X. L. Characterization of natural sphalerite as a novel visible-light-driven photocatalyst. *Solar Energy Mater. Solar Cells* **2008**, *92* (8), 953−959.

(4) Li, Y.; Lu, A. H.; Jin, S.; Wang, C. Q. Photo-reductive decolorization of an azo dye by natural sphalerite: Case study of a new type of visible light-sensitized photocatalyst. *J. Hazard. Mater.* **2009**, *170* (1), 479−486.

(5) Yang, X. G.; Li, Y.; Lu, A. H.; Yan, Y. H.; Wang, C. Q.; Wong, P. K. Photocatalytic reduction of carbon tetrachloride by natural

sphalerite under visible light irradiation. *Solar Energy Mater. Solar Cells* **2007**, *95* (7), 1915−1921.
(6) Chen, Y. M.; Lu, A. H.; Li, Y.; Zhang, L. S.; Yip, H. Y.; Zhao, H. J.; An, T. C.; Wong, P. K. Naturally occurring sphalerite as a novel cost-effective photocatalyst for bacterial disinfection under visible light. *Environ. Sci. Technol.* **2011**, *45* (13), 5689−5695.
(7) Chen, Y. M.; Lu, A. H.; Li, Y.; Yip, H. Y.; An, T. C.; Li, G. Y.; Jin, P.; Wong, P. K. Photocatalytic inactivation of *Escherichia coli* by natural sphalerite suspension: Effect of spectrum, wavelength and intensity of visible light. *Chemosphere* **2011**, *84* (9), 1276−1281.
(8) Polshettiwar, V.; Luque, R.; Fihri, A.; Zhu, H. B.; Bouhrara, M.; Basset, J. M. Magnetically revoverable nanocatalysts. *Chem. Rev.* **2011**, *111* (5), 3036−3075.
(9) Kostedt, W. L.; Drwiega, J.; Mazyck, D. W.; Lee, S. W.; Sigmund, W.; Wu, C. Y.; Chadik, P. Magnetically agitated photocatalytic reactor for photocatalytic oxidation of aqueous phase organic pollutants. *Environ. Sci. Technol.* **2005**, *39* (20), 8052−8056.
(10) Zhang, L.; Wang, W. Z.; Zhou, L.; Shang, M.; Sun, S. M. Fe_3O_4 coupled BiOCl: A highly efficient magnetic photocatalyst. *Appl. Catal. B: Environ.* **2009**, *90* (3−4), 458−462.
(11) Barmatova, M. V.; Ivanchikova, I. D.; Kholdeeva, O. A.; Shmakov, A. N.; Zaikovskii, V. I.; Mel'gunov, M. S. Magnetically separable titanium-silicate mesoporous materials with core−shell morphology: Synthesis, characterization and catalytic properties. *J. Mater. Chem.* **2009**, *19* (39), 7332−7339.
(12) Beydoun, D.; Amal, R.; Low, G.; McEvoy, S. Novel photocatalyst: Titania-coated magnetite. Activity and photodissolution. *J. Phys. Chem. B.* **2000**, *104* (18), 4387−4396.
(13) Leung, T. Y.; Chan, C. Y.; Hu, C.; Yu, J. C.; Wong, P. K. Photocatalytic disinfection of marine bacteria using fluorescent light. *Water Res.* **2008**, *42* (19), 4827−4837.
(14) Saito, T.; Iwase, T.; Horie, J.; Morioka, T. Mode of photocatalytic bactericidal action of powdered semiconductor TiO_2 on mutans streptococci. *J. Photochem. Photobiol. B* **1992**, *14* (4), 369−379.
(15) Kiwi, J.; Nadtochenko, V. Evidence for the Mechanism of Photocatalytic degradation of the bacterial wall membrane at the TiO_2 interface by ATR-FTIR and kinetic fast spectroscopy. *Langmuir* **2005**, *21* (10), 4631−4641.
(16) Nadtochenko, V.; Rincon, A.; Stanka, S.; Kiwi, J. Dynamics of *E. coli* photokilling due to cell wall lysis during TiO_2 photocatalysis. *J Photochem. Photobiol. A.* **2005**, *169* (2), 131−137.
(17) Bacsa, R.; Kiwi, J.; Ohno, T.; Albers, P.; Nadtochenko, V. Preparation, testing and characterization of doped TiO_2 active in the peroxidation of biomolecules under visible light. *J. Phys. Chem. B.* **2005**, *109* (12), 5994−6003.
(18) Maness, C. P.; Smolinski, S.; Blake, D. M.; Huang, Z.; Wolfrum, E. J.; Jacoby, W. A. Bactericidal activity of photocatalytic TiO_2 reaction: Toward and understanding of its killing mechanism. *Appl. Environ. Microbiol.* **1999**, *65* (9), 4094−4098.
(19) Zhang, L. S.; Wong, K. H.; Yip, H. Y.; Hu, C.; Yu, J. C.; Chan, C. Y.; Wong, P. K. Effective photocatalytic disinfection of *E. coli* K-12 using AgBr-Ag-Bi_2WO_6 nanojunction system irradiated by visible light: The role of diffusing hydroxyl radicals. *Environ. Sci. Technol.* **2010**, *44* (4), 1392−1398.
(20) Li, G. Y.; Liu, X. L.; Zhang, H. M.; An, T. C.; Zhang, S. Q.; Carroll, A. R.; Zhao, H. J. In situ photoelectrocatalytic generation of bactericide for instant inactivation and rapid decomposition of Gram-negative bacteria. *J. Catal.* **2011**, *277* (1), 88−94.
(21) Li, Y.; Lu, A. H.; Wang, C. Q. Photocatalytic reduction of Cr(VI) by natural sphalerite suspensions under visible light irradiation. *Acta Geol. Sin.* **2006**, *80* (2), 267−272.
(22) Cullity, B. D.; Graham, C. D. *Introduction to Magnetic Materials*, 2nd ed.; Wiley-IEEE Press: NJ, 2009.
(23) Rawat, J.; Rana, S.; Srivastava, R.; Misra, R. D. K. Antimicrobial activity of composite nanoparticles consisting of titania photocatalytic shell and nickel ferrite magnetic core. *Mater. Sci. Eng., C* **2007**, *27* (3), 540−545.
(24) Dunstan, D. E.; Hagfeldt, A.; Almgren, M.; Siegbahm, H. O. G.; Mukhtar, E. Importance of surface reactions in the photochemistry of zinc sulfide colloids. *J. Phys. Chem. C.* **1990**, *94* (17), 6797−6804.
(25) Tang, W. Z.; Huang, C. P. Inhibitory effect of thioacetamide on CdS dissolution during photocatalytic oxidation of 2,4-dichlorophenol. *Chemosphere* **1995**, *30* (7), 1385−1399.
(26) Buxton, G. V.; Greenstock, C. L.; Helman, W. P.; Ross, A. B.; Tsang, W. Critical review of rate constants for reactions of hydrated electrons, hydrogen atoms and hydroxyl radicals in aqueous Solution. *J. Phys. Chem. Ref. Data* **1988**, *17* (2), 513−886.
(27) Vanhemmen, J. J.; Meuling, W. J. A. Inactivation of *Escherichia coli* by superoxide radicals and their dismutation products. *Arch. Biochem. Biophys.* **1977**, *182* (2), 743−748.
(28) Cho, M.; Snow, S. D.; Hughes, J. B.; Kim, J. H. *Escherichia coli* inactivation by UVC-irradiated C60: Kinetics and mechanisms. *Environ. Sci. Technol.* **2011**, *45* (22), 9627−9633.
(29) Abbas, M. E.; Luo, W.; Zhu, L.; Zou, J.; Tang, H. Fluorometric determination of hydrogen peroxide in milk by using a Fenton reaction system. *Food Chem.* **2010**, *120* (1), 327−331.
(30) Ranjit, K. T.; Willner, I.; Bossmann, S. H.; Braun, A. M. Lanthanide oxide-doped titanium dioxide photocatalysts: Novel photocatalysts for the enhanced degradation of *p*-chlorophenoxyacetic acid. *Environ. Sci. Technol.* **2001**, *35* (7), 1544−1549.
(31) Sakai, H.; Baba, R.; Hashimoto, K.; Fujishima, A. Local detection of photoelectrochemically produced H_2O_2 with a "wired" horseradish peroxidase microsensor. *J. Phys. Chem.* **1995**, *99* (31), 11896−11900.
(32) Kikuchi, Y.; Sunada, K.; Iyoda, T.; Hashimoto, K.; Fujishima, A. Photocatalytic bactericidal effect of TiO_2 thin films: Dynamic view of the active oxygen species responsible for the effect. *J. Photochem. Photobiol. A: Chem.* **1997**, *106* (1−3), 51−56.